Journal of Polymers and the Environment (2018) 26:2793–2802
https://doi.org/10.1007/s10924-017-1162-7

ORIGINAL PAPER

Effects of UV/Photo-Initiator Treatments on Enhancement of Crystallinity of Polylactide Films and Their Physicochemical Properties

Mijanur Rahman[1] · **Pakorn Opaprakasit**[1]

Published online: 18 December 2017
© Springer Science+Business Media, LLC, part of Springer Nature 2017

Abstract
Effects of UV/photo-initiator treatments on crystal formation and properties of polylactide (PLLA) films are investigated. Camphorquinone and riboflavin photo-initiator solutions in methanol are employed in the treatment of amorphous quenched PLLA films. Results from FTIR, ATR-FTIR, DSC, XRD, and SEM show evidence of crystalline domain formation dispersed throughout the film. ^{1}H NMR and GPC results suggest that the molecular weights of the polymer slightly decrease after the treatment. This indicates that the treatment leads to a diffusion of the photo-initiators molecules through the film matrix, resulting in a low degree of PLLA chain scissions, and formation of carboxylic acid and hydroxyl polar end groups. This, in turn, induces PLLA crystallization, which imposes profound effects on surface wettability and physical and mechanical properties of the samples. The process can be applied in optimizing properties of PLLA films with shorter treatment times, compared to other methods, which is suitable for use in various fields; especially those that require specific characteristics like biomedical, packaging and environmental applications.

Keywords Polylactide · Photo-initiator · Crystallization · Glass transition temperature (T_g) · Tensile test

Introduction

In recent times, consumption volumes of biopolymers are growing tremendously. Among these, polylactide, PLLA, a thermoplastic aliphatic polyester, is one of the most popular. The material is derived from lactic acid, obtained from microbial fermentation of renewable agricultural raw materials [1–3]. PLLA exhibits various outstanding properties; such as biodegradability, biocompatibility, easy processability, good mechanical properties, and low carbon emission during its production [4–7]. The materials is widely used in biomedical and environment-friendly (as an alternative to petrochemical-based plastics) applications [8–10], for example, in drug delivery systems, nanofibers tissue scaffold, implant devices for bone fixation, industrial packaging materials, paper coatings, films, and sustained release systems for pesticides and fertilizers [11–15].

To extend its application areas, many researchers have studied oxidative, hydrolytic, and enzymatic properties, thermal degradation, and crystallization behaviors of PLLA-based materials [16–27]. For biomedical applications, effects of gamma, beta, and laser radiations on PLLA-based materials have been investigated [28–31]. Although many PLLA materials used in outdoor applications are directly exposed to ultraviolet (UV) radiation, only a few recent works have been reported regarding the effects of UV light on properties deterioration and degradability of the materials [32–36]. Copinet et al. [32] reported that degradation rate of PLLA was enhanced by UV treatment, reflected by a rapid decrease in its weight-average molecular weight, glass transition temperature (T_g), and elongation at break. Yasuda et al. [33] reported a faster reduction of molecular weight, along with a gradual loss of optical purity in PLLA chains under UV–C irradiation. Recent work performed on PLLA–TiO_2 nanocomposites films revealed that both accelerating and shielding effects of UV irradiation were observed, mainly depending on the method of composite preparation [34–36]. To the

✉ Pakorn Opaprakasit
pakorn@siit.tu.ac.th

Mijanur Rahman
muhin676@gmail.com

[1] School of Biochemical Engineering and Technology, Sirindhorn International Institute of Technology (SIIT), Thammasat University, Pathum Thani 12121, Thailand

best of our knowledge, there has been no quantitative study, along with in-depth qualitative research on the impact of UV irradiation on structures and properties of PLLA films in the presence of photo-initiators.

In this work, effects of treatments by two photo-initiator solutions under UV light on crystallinity enhancements of PLLA films are investigated. Camphorquinone and riboflavin photo-initiators are employed. Mechanisms of this crystallization enhancement and its effects on the material properties are examined, in terms of molecular structures, morphology, thermal properties, surface properties, and mechanical behaviors. The process can be further applied in modifications of PLLA properties for various applications; especially those that require specific characteristics like biomedical, packaging and environmental applications.

Experimental

Materials

Commercial poly(L-lactide), PLLA, was purchased from NatureWorks Co. Ltd. (USA). Riboflavin (RF) photo-initiator and *N,N,N′,N′*-tetramethylethylenediamine (TEMED) co-initiator (Acros, Thermo Fisher Scientific, USA), ammonium persulfate (APS) RPE-ACS (Carlo) thermal-initiator, camphorquinone (CQ) photo-initiator (Esstech Inc., USA), and *N,N′*-dimethylaminoethyl methacrylate co-initiator (Fluka, USA) were used as received. Commercial grade methanol (MeOH) and ethanol (EtOH) solvents (Italmar co., Ltd., Thailand) and deionized water (DI water) were used throughout this work.

Sample Preparations

PLLA films were prepared in a Compression Molding Machine (model PR2D-W300L300HD-WCL, Chareontut, Thailand) by placing pellets (6.5–7.0 g) between two stainless steel plates lined with PET transparency films. The samples were pressed at 190 °C for 14 min at a pressure of 2150 psi, and then cooled down to room temperature. The average thickness of the resulting films was 0.22 mm.

UV-induced crystallization (and slight degradation) of PLLA films were investigated by employing photo-initiator solutions, prepared by dissolving 0.1 g of initiator(s) and 0.1 mL of co-initiator in 100 mL MeOH solvent. Two different initiator(s)/co-initiator systems, i.e., CQ/DMAEMA and RF-APS/TEMED were employed. In the treatment process, PLLA films were first surface activated by UV light (254 nm) at room temperature for 20 min, using a Spectronics Corp., USA model: ENF-260C/FE. The films passed through this process are defined as irradiated PLLA films.

To examine UV-induced crystallization behaviors, 20 mL of a specific initiator solution was poured to completely cover the UV-activated films in a petri dish. The samples were then further irradiated under UV light for 20 min. After that, the samples were intensely washed with DI water and then EtOH to remove residual chemicals. The films passed through the treatment using the CQ-system are defined as CQ-treated PLLA, and those using the RF-system are noted as RF-treated PLLA. All films were finally dried in a vacuum oven at 40 °C for 48 h, and kept in a desiccator for further characterization.

Characterizations

Changes in molecular weights and molecular weight distributions ($\overline{Mn}$, $\overline{Mw}$ and PDI) of PLLA films before and after treatments were examined by gel permeation chromatography (GPC) on a Waters 150-CV gel permeation chromatograph. THF was used as the solvent with a flow rate of 1 mL/min. Mono-dispersed polystyrene was employed as a standard. X-ray diffraction (XRD) was conducted on a JEOL JDX-3530 diffractometer, using a monochromatic Cu Kα X-ray source at 40 kV and 30 mA. The samples were scanned from 2θ of 5°–30° with a 0.02 step size. Thermal behaviors of the films were observed by differential scanning calorimetry (DSC) on a DSC822^e (Mettler Toledo Instruments). The samples were scanned with a double cycle of heating from − 20 to 170 °C at a heating/cooling rate of 10 °C/min, under N_2 atmosphere of 60.0 mL/min.

Cross-sectional topography of the films was examined by scanning electron microscopy (SEM), using a Hitachi SU8000 scanning microscope. The films were broken down with the aid of liquid nitrogen and mounted on adhesive carbon black on metal stubs. The samples were dried in a vacuum oven at 40 °C overnight and sputter-coated with a 10 nm gold layer for cross-sectional observation. Chemical structures and interaction of the samples were investigated using fourier transform infrared (FTIR) spectroscopy on a Thermo Scientific Nicolet iS5, equipped with iD1 transmission and iD5 attenuated total reflectance (ATR) (diamond crystal) accessories. All spectra were recorded with 64 scans at a 2 cm^{-1} resolution. ^{1}H nuclear magnetic resonance (^{1}H NMR) spectroscopy was used to examine the polymer's microstructures and the origin of crystallization. The spectra were taken on an AVENCE 300 MHz digital NMR spectrometer (Bruker Biospin; DPX-300, Rheinstetten, Germany) using deuterated chloroform ($CDCl_3$) as a solvent.

Tensile properties of the films were measured using a universal tensile machine (Tinius Olsen Bench Machine: model H5K-T UTM), according to ASTM D882-10, with a crosshead speed of 50 mm/min, using rectangle-shaped specimens with 50 mm gauge length and 15 mm width. The average values of at least 10 specimens for each batch of

samples were used. Surface hydrophilicity of the films was analyzed through a water droplet contact angle at pH 4, 7, and 10. At least ten repetitions were measured and reported for each sample.

Results and Discussion

Effects of UV irradiation on degradation of PLLA chains are first examined. GPC chromatograms of neat PLLA in comparison with a CQ-treated sample, provided as supporting data, show a slight shift of the distribution peak toward longer elution time, with no apparent secondary peak. The results on average molecular weights, as summarized in Table 1, indicate a decrease of both $\overline{Mn}$ and $\overline{Mw}$ of about 10 and 16%, respectively, after the treatment. This reflects degradation of PLLA chains during the CQ-treated process. The Polydispersity Index (PDI) remains significantly unchanged, suggesting that chain scissions occurred randomly along the polymer chains.

It is clearly observed that after the treatments, both treated PLLA films became opaque (almost completely white), whereas neat PLLA and irradiated PLLA films remained transparent. This is likely due to differences in crystalline structures of the samples. To verify this, all film specimens were characterized by XRD. Both neat PLLA and irradiated films show a broad amorphous halo with a very weak diffraction peak at 16.8°, as shown in Fig. 1. This reflects that UV radiation alone has no effect on promoting the crystallization of PLLA. In contrast, the corresponding spectra of CQ-treated and RF-treated films show three sharp signals at 14.7°, 16.5°, 18.9°, and 22.2°, corresponding to (010), (110)/(200), (203), and (205) planes of the α-crystalline form [19, 35]. This indicates much higher crystallinity of the treated films.

Table 1 GPC results of average molecular weights of neat and CQ-treated PLLA samples

Samples	$\overline{Mn}$	$\overline{Mw}$	PDI
Neat PLLA	95,820	200,340	2.1
CQ-treated PLLA	86,140	168,210	2.0

The neat and irradiated PLLA films exhibit roughly 2% crystallinity, whereas a drastic increase in the values to 34.8 and 37.3% is observed for the CQ-treated and RF-treated PLLA films. This implies that the original film is almost completely amorphous, as it is quenched after the compression process. The UV-irradiated treatment without photo-initiator does not promote crystallization, while the CQ and RF treatments can induce formation of semi-crystalline structures. In other words, crystallization of PLLA can be initiated by UV/photo-initiator treatments at room temperature, at a much shorter time (shorter than 40 min), compared to other processes, such as annealing.

Effects of photo-initiator treatments on thermal properties of PLLA films are studied, in which their DSC thermograms are shown in Fig. 2, and the results are summarized in Table 2. The glass transition temperature (T_g), melting temperature (T_m), and the degree of crystallinity (X_c), are measured separately from both 1st and 2nd heating thermograms. In the calculation of crystallinity (%), the enthalpy of fusion per mole of PLLA of the infinite size perfect crystal of 93.0 J/g, is employed [37].

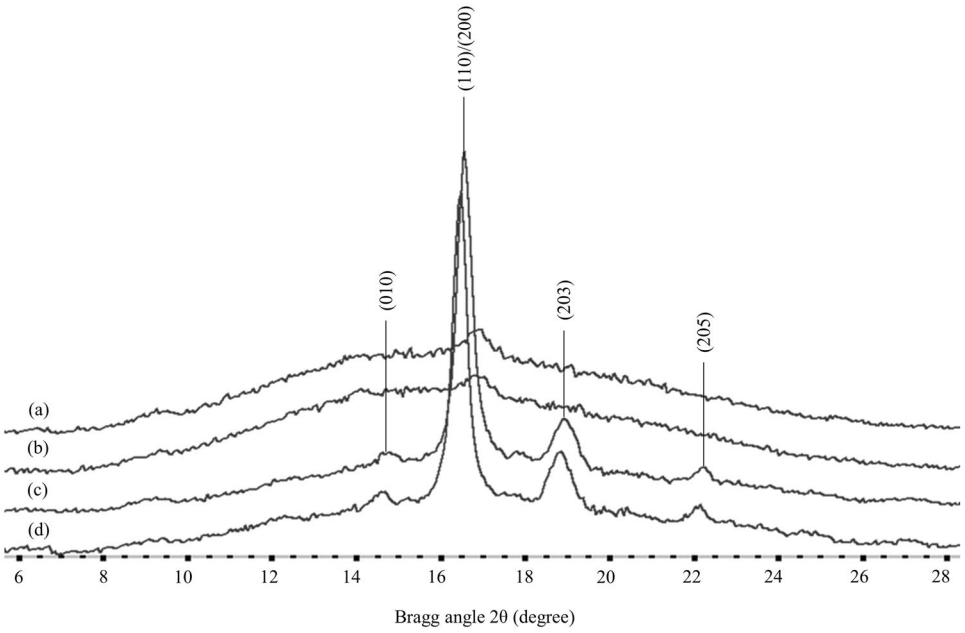

Fig. 1 XRD diffractograms of neat PLLA (*a*), irradiated PLLA (*b*), CQ-treated PLLA (*c*), and RF-treated PLLA (*d*) films

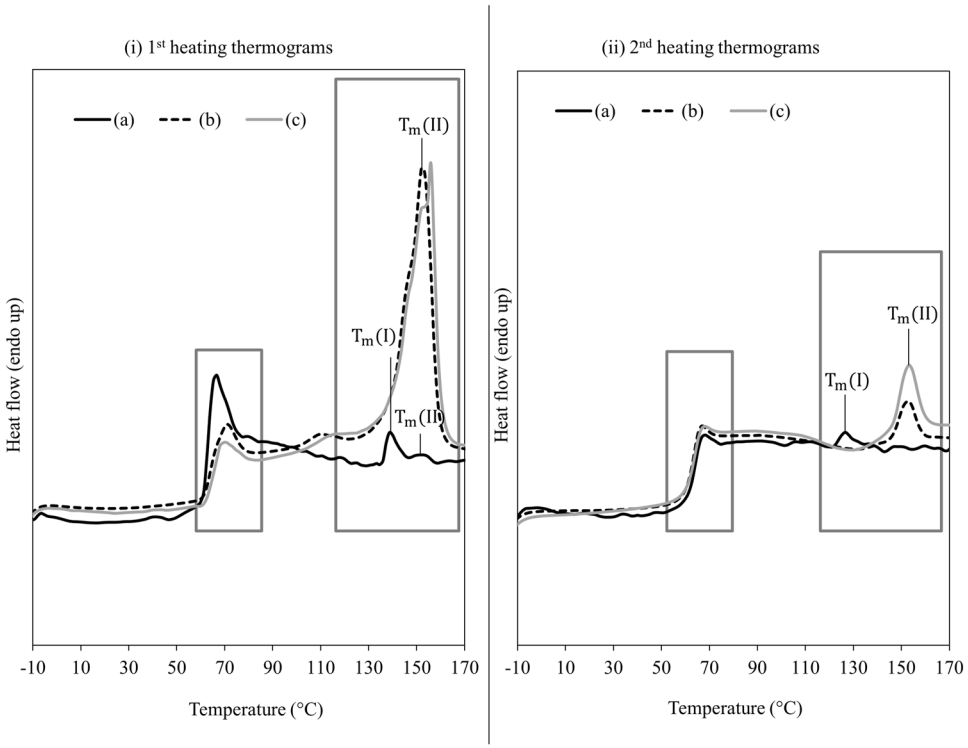

Fig. 2 DSC 1st and 2nd heating thermograms of neat PLLA (*a*), CQ-treated PLLA (*b*), and RF-treated PLLA (*c*) films

Table 2 Thermal properties derived from 1st and 2nd heating DSC thermograms of neat PLLA, CQ-treated PLLA, and RF-treated PLLA films

Samples	1st heating cycle				2nd heating cycle		
	T_g (°C)	T_m(II) (°C)	T_m(II) (°C)	X_c (%)	T_g (°C)	T_m(II) (°C)	X_c (%)
Neat PLLA	62.3	138.7	153.7	1.5	62.7	126.7	0.6
CQ-treated PLLA	64.4	146.7	152.7	26.0	63.5	152.7	2.9
RF-treated PLLA	65.8	146.7	152.7	27.2	63.6	153.3	4.3

The treated films have higher T_g and crystalline contents, compared to neat PLLA in both 1st and 2nd heating cycles. The 1st scan data provides information on the actual crystalline state of the samples. As a result of the treatment, the crystallinity increases up to 24.2 and 25.3% in the CQ-treated and RF-treated PLLA films, respectively, from 1.5% of the starting neat PLLA. This reflects a remarkable transformation of the amorphous region into crystalline domains through the treatments. With the aid of methanol solvent penetration into the bulk of PLLA matrix, initiator/co-initiator promotes PLLA chain scission under UV irradiation. The newly-formed carboxylic acid and hydroxyl end groups trigger crystallization process simultaneously. The simultaneous chain scission and crystallization process is termed as chemicrystallization [16]. As the crystallinity increases, the movements of chain segments become constrained, reflecting the increase in T_g, from 62.3 °C in neat PLLA, to 64.4 and 65.8 °C in the CQ-treated and RF-treated PLLA films.

It is also observed that in the 1st heating thermograms, double melting endotherms, T_m(I) and T_m(II) are clearly detected in neat PLLA film at 138.7 and 153.7 °C. However, in the treated films, the 1st peak resolved as a shoulder at 146.7 °C of a strongly noticeable 2nd peak at 152.7 °C. These two endotherms in neat PLLA are related to the melting of two distinct initial crystalline structures of PLLA, i.e., the disordered α′ crystalline form and ordered α crystalline form, respectively [27, 38, 39]. The less stable α′ form is likely a result from low degree crystallization during the UV treatment. Aging behavior is observed as an endotherm after the glass transition. This indicates that the chains are attempting to crystallize, however, restriction of chain movements leads to incomplete formation of crystalline domains. In CQ-treated and RF-treated PLLA films, a much higher amount of ordered α crystal is formed, which induce crystallization of the chains.

Unlike the 1st heating scans, the corresponding thermograms from the 2nd heating cycle show the crystallization behavior of PLLA chains, regardless of their thermal history. A single melting peak T_m is observed in all samples. Neat PLLA shows only a weak α′ melting peak, indicating that the applied cooling rate is not slow enough for crystalline formation. The treated samples, however, show α form crystals,

which can be formed during these DSC experiments, indicating the presence of effective crystallization nucleation. The T_g value and crystallinity also slightly increase in the 2nd heating cycle for the treated films. From neat PLLA to treated samples, T_g increases approximately 1 °C, due to the formation of crystalline domains and strong specific interactions (likely hydrogen bonding) induced by the newly-generated end groups, which can act as physical crosslinks in restricting chain segmental movements.

SEM micrographs, as shown in Fig. 3, illustrate the cross-sectional morphology of treated films. Profound changes are clearly observed, in which a transition from amorphous structure to semi-crystalline domains is reflected as white areas dispersed throughout the matrix. This is evidence that a transformation has taken place because of chemicrystallization of the PLLA chains during the treatments. In addition, the results suggest that crystalline domains are not only confined at the edges of the treated films, but also spread over the whole cross-sectional area. The CQ-treated film has large crystalline domains, approximately 2 μm, with lower density, while the corresponding RF-treated film shows densely populated domains, but with much smaller sizes.

Crystallization mechanisms and interactions are characterized by FTIR spectroscopy. Figure 4(i) shows transmission spectra of the O–H stretching and C=O overtone modes, in which difference spectra of all treated samples after subtraction of the neat PLLA characteristics are also shown. Both treated samples show a distinct sharp O–H stretching band at 3294 cm^{-1}. This is not observed in the irradiated PLLA spectrum, suggesting that it originates from the photo-initiator treating process, likely -OH of isolated carboxylic acids. The C=O overtone bands also occur in this region, whose band characteristics are strongly dependent on the carbonyl environment and interactions [24, 40]. The splitting patterns of bands at 3646, 3561 and 3510 cm^{-1} of the treated-neat PLLA (c-a and d-a) are clearly different from that of the corresponding irradiated-neat PLLA (b-a) spectrum. This firmly indicates the formation of hydrogen bonding interactions, as a result from extra crystalline formation.

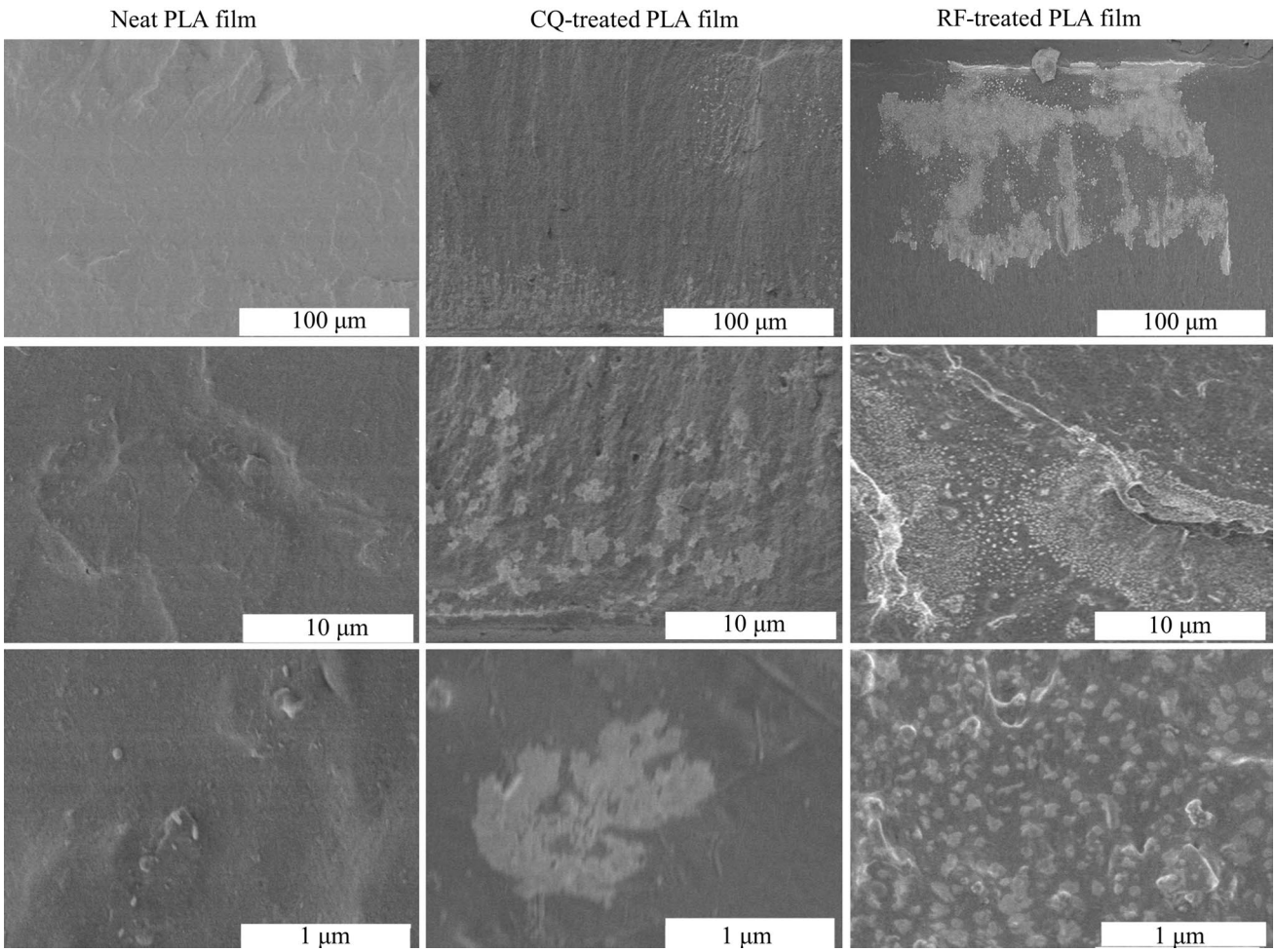

Fig. 3 Cross-sectional SEM micrographs of neat PLLA, CQ-treated PLLA, and RF-treated PLLA films, at different magnifications

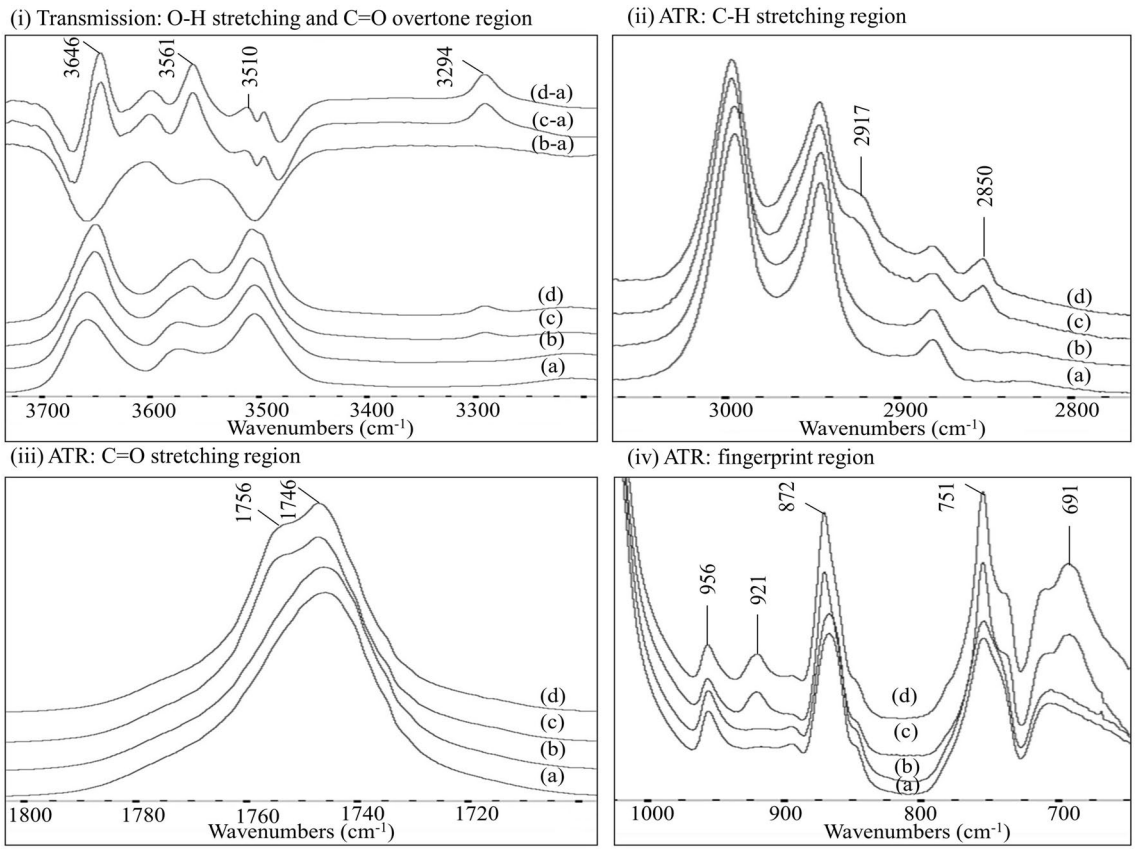

Fig. 4 FTIR spectra measured in transmission mode (**i**) of neat PLLA (*a*), irradiated PLLA (*b*), CQ-treated PLLA (*c*), and RF-treated PLLA (*d*) films, and their difference spectra after subtraction of neat PLLA characteristics. ATR-FTIR spectra of the corresponding samples in the C–H stretching (**ii**), the C=O stretching (**iii**) and finger print (**iv**) regions

ATR-FTIR spectra in the C–H stretching region of the films are shown in Fig. 4(ii). The neat and irradiated PLLA show bands at 2995 and 2945 cm^{-1} aroused from asymmetric and symmetric stretching of $–CH_3$ groups, and at 2880 cm^{-1} from the stretching of –C–H bonds of PLLA. The intensity of these bands slightly decreases in the treated samples, and two new C–H stretching bands are developed at 2917 and 2850 cm^{-1} [17]. These findings are indicative of slight degradation of PLLA chains. It is noted that these two bands may be associated with residual methanol solvent in the film matrix.

Figure 4(iii) shows characteristic C=O modes of PLLA, which are sensitive to chain conformation and interactions. After treatments, the 1746 cm^{-1} band splits into two bands at 1746 and 1756 cm^{-1}. Rasselet [16] reported that the band at 1756 cm^{-1} is attributed to the lowest energy gauche-trans (gt) conformation of the crystal structure, whereas the 1746 cm^{-1} mode is due to the trans–trans (tt) conformation of the amorphous domains [26]. Bocchini et al. [17] and Gardette et al. [41] identified a C=O band at 1845 cm^{-1} when PLLA was oxidized by UV irradiation. However, no such band is observed in the spectra of our treated samples, indicating these treated films experienced a much less severe degradation mechanism.

The appearance of a band at 921 cm^{-1} and splitting of bands at 751 and 691 cm^{-1} are direct indicative of PLLA's crystalline formation [16, 42]. Figure 4iv illustrates that neat and irradiated PLLA show only a weak band at 921 cm^{-1}, whereas the band intensity of this mode becomes very strong in both treated samples. The 751 and 691 cm^{-1} bands also become sharper and show a splitting pattern. The results firmly indicate the formation of crystalline domains. In addition, the relative intensity of the 921/956 cm^{-1} mode from both transmission (not shown) and ATR spectra are comparable. Given that the penetration depth of ATR measurement is around 200 μm from the surface, while the transmission spectra show absorption characteristics of the bulk film, the newly-formed crystalline domains are dispersed throughout the films, not concentrated only at the film's surface.

^1H NMR analysis is used to study the polymer's microstructures. The spectra of neat PLLA and CQ-treated samples are shown in Fig. 5. Three characteristic signals of PLLA are observed in both neat PLLA and CQ-treated sample. The signals of lactate methyl (H^a) and methine protons

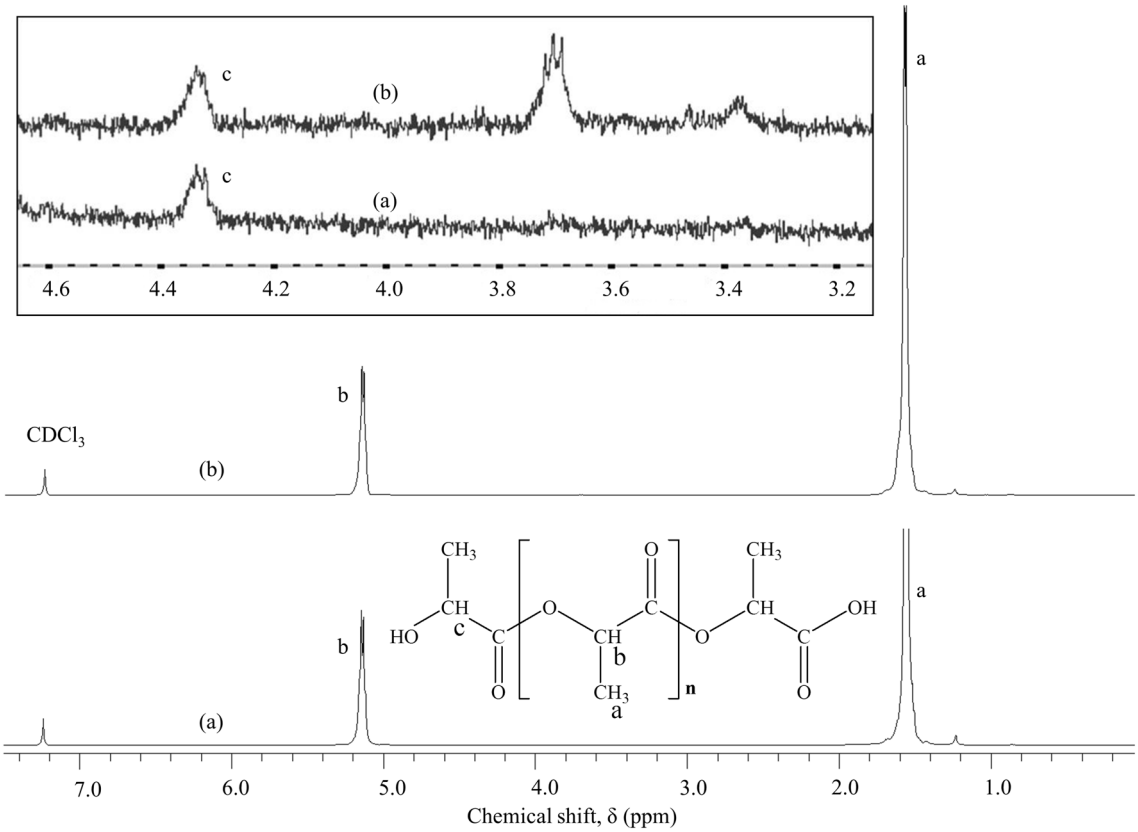

Fig. 5 ^{1}H NMR spectra of neat PLLA (*a*), and CQ-treated PLLA (*b*) films

(H^b) are located at 1.5–1.7 and 5.1–5.2 ppm, whereas a weak peak at 4.3–4.4 ppm (inset) is accounted for the chain end methine protons (H^c) [43]. Besides these, there are two additional signals at around 3.4 and 3.7 ppm in the CQ-treated PLLA spectrum (inset). These are identified as methylene of ethanol (used to wash the treated film) and methyl protons of methanol solvent [44]. The presence of these peaks reflects that during the treatment, methanol molecules play a significant role in penetrating the films and facilitate the diffusion of the initiator molecules, to induce the nucleation stage of crystallization. After crystallization, however, trace amounts of these molecules may still remain in the sample. It is noted that without photo-initiators, these alcohol molecules cannot initiate the crystallization. Most importantly, no other spectral characteristics can be detected, and the calculated values of the lactate repeat units (H^b/H^c) of neat PLLA and the treated samples are similar. This ensures that a slight degree of chain scissions occurs, which in turn play a key role in promoting crystallization.

To examine the mechanical properties of the treated samples, stress–strain curves of neat PLLA, CQ-treated PLLA, and RF-treated PLLA films are compared in Fig. 6(i). All three films exhibit semi-crystalline behavior, in which a yield point is observed before breaking of the samples. Results on tensile properties are summarized in Fig. 6(ii, iii). The tensile strength and modulus decrease moderately from neat PLLA (62.4 MPa) to treated PLLA samples (56.9 and 58.0 MPa for the CQ-treated and RF-treated PLLA films, respectively). This may be directly related to the slight chain scissions taking place during film treatments. The modulus also decreases as a function of the treatments from 1.91 GPa to 1.86 and 1.88 GPa for the CQ-treated and RF-treated samples, respectively. This is explained by the generation of micro-voids during the methanol solvent penetration into the film matrix. Although, enhancement in crystallization is observed, but there may be other drawbacks.

In contrast, the elongation at break of neat PLLA film (4.6%) increases modestly to 5.6 and 5.5%. The break energy values also increase from 1.7 to 2.1 and 2.0 TJ/m^3, respectively. This is likely a result of the formation of crystalline domains and strong hydrogen bonding, induced by more –OH and –COOH chain ends. It is noted that chain movements during the treatment process, allow the relaxation of stress that was imposed on the films during the preparation step, which may affect the enhancement of these properties.

Surface properties of the film samples before and after treating with photo-initiator solutions are examined. Results for water contact angle, measured at room temperature

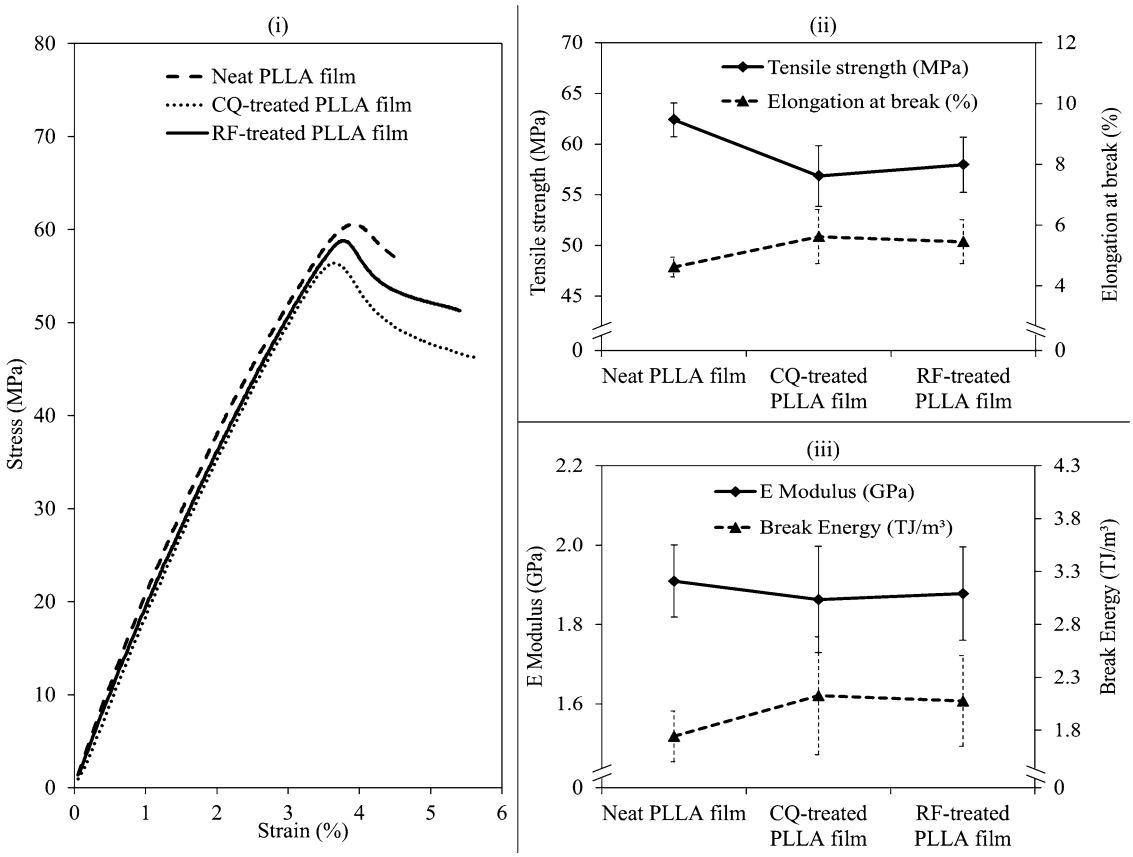

Fig. 6 Stress versus strain behavior (**i**) of neat PLLA, CQ-treated PLLA, and RF-treated PLLA films. The results on tensile strength, elongation at break (**ii**) and break energy, E modulus (**iii**) of neat PLLA, CQ-treated PLLA, and RF-treated PLLA films

(using water droplets at pH of 4, 7 and 10), of neat PLLA and treated samples, are summarized in Fig. 7. Neat PLLA and irradiated films show comparable surface wettability, reflected by a similar contact angle of ~68°. This strongly agrees with other results previously discussed that minimal structural changes occur, especially at the surface, when the film is only treated by UV without the photo-initiators. For the same film samples, the values slightly increase with an increase in pH of the water droplets, reflecting the slight negatively-charged nature of the surface.

The UV/initiator treated PLLA films, however, have much lower contact angle values, compared to the initial neat PLLA, indicating their more hydrophilic surface. When water droplets at pH of 7 are employed, values of 65.7° and 64.5° are observed for the CQ-treated and RF-treated PLLA films, respectively. More remarkable decreases to 63.9° and 63.6° are obtained when acidic water is used. This is likely due to the presence of newly-generated polar end groups from chain scissions. Also, for the same treated sample, the contact angle markedly increases with an increase in pH of the water droplets. This strongly confirms that the treated film surfaces are negatively charged, due to high contents of terminal –OH, –COOH, and carboxylate derivatives.

It is worth to mention that the remaining initiators in the treated films may play some roles on the properties of the treated films. To verify this, a standard quantitative technique for evaluation of the initiators contents in the treated films has been developed. The results confirm that at the applied concentration, only trace amounts of photo-initiators remain on the treated films. However, when the concentration of the photo-initiators is increased, a significant increase in the crystallinity of the treated PLLA films is observed. Detailed investigation into this will be reported in a separate publication.

Conclusions

The application of UV/photo-initiators treatments to PLLA films leads to an enhancement in crystalline content of the amorphous quenched films. The results from FTIR, ATR-FTIR, DSC, XRD, and SEM show evidence of crystalline domains formation throughout the film matrix, not limited to the film surface. The molecular weights of the polymer slightly decrease after the treatment. In contrast, the use of only UV light does not show any noticeable changes in

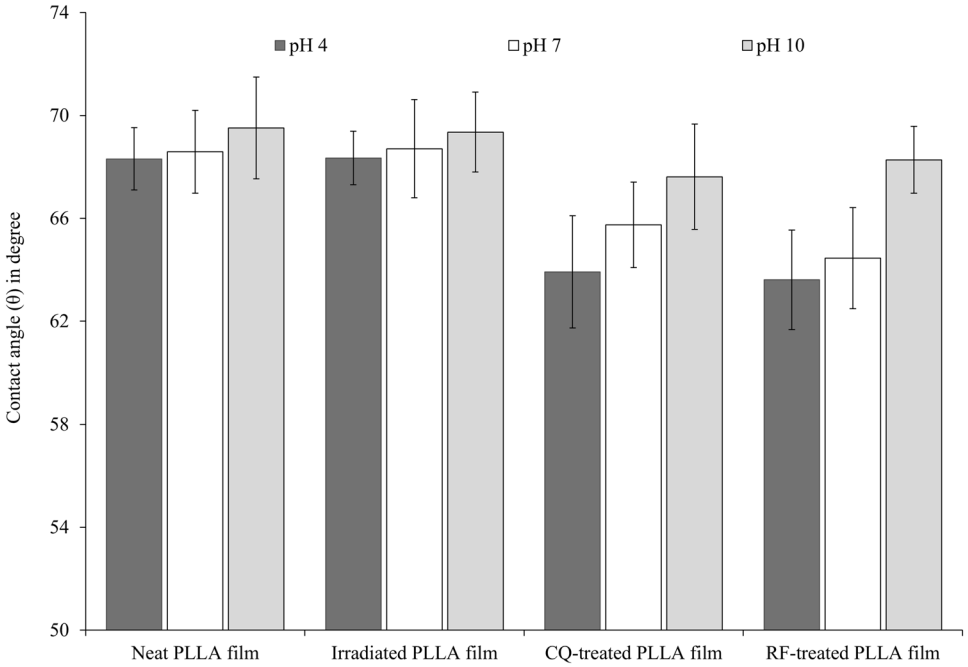

Fig. 7 Water contact angle, using water droplets at various pH values, of neat PLLA, irradiated PLLA, CQ-treated PLLA, and RF-treated PLLA films

properties of the films. It is, therefore, concluded that the treatment leads to a diffusion of the photo-initiators molecules through the film matrix, facilitated by solvent molecules. This results in a low degree of chain scissions, generating carboxylic acid and hydroxyl polar end groups, which in turn act as nucleating agents to induce crystallization of PLLA chains. Both CQ and RF photo-initiators undergo similar mechanisms, with slight differences in sizes of their visible domains. These induced crystalline domains impose profound effects on surface wettability and the physical and mechanical properties of the samples. The process can be applied in optimizing properties of PLLA films with shorter treatment times, compared to other methods, suitable for use in various applications.

Acknowledgements The authors acknowledge financial support from the National Research University (NRU) grant, provided from The Office of Higher Education Commission (OHEC), the Thammasat University Research Fund (Theme research), and the Center of Excellence in Materials and Plasma Technology (CoE M@P Tech), Thammasat University. Mijanur Rahman thanks the support from the Graduate Scholarship Program for Excellence Foreign scholarship (EFS) by SIIT.

References

1. Garlotta D (2001) J Polym Environ 9:63–84
2. Hartmann MH (1998) In: Kaplan DL (ed) Biopolymers from renewable resources. Springer, Berlin, pp 367–411
3. Auras RA, Lim LT, Selke SEM, Tsuji H (2011) Poly(lactic acid): synthesis, structures, properties, processing, and applications. Wiley, New Jersey
4. Tokiwa Y, Calabia BP (2006) Appl Microbiol Biotechnol 72:244–251
5. Fukushima K, Abbate C, Tabuani D, Gennari M, Camino G (2009) Polym Degrad Stab 94:1646–1655
6. Leenslag JW, Pennings AJ, Bos RRM, Rozema FR, Boering G (1987) Biomaterials 8:311–314
7. Lim JY, Kim SH, Lim S, Kim YH (2003) Macromol Mater Eng 288:50–57
8. Nampoothiri KM, Nair NR, John RP (2010) Bioresour Technol 101:8493–8501
9. Jamshidian M, Tehrany EA, Imran M, Jacquot M, Desobry S (2010) Compr Rev Food Sci Food Saf 9:552–571
10. Drumright RE, Gruber PR, Henton DE (2000) Adv Mater 12:1841–1846
11. Kumari A, Yadav SK, Yadav SC (2010) Colloids Surf B 75:1–18
12. Sun Z, Zussman E, Yarin AL, Wendorff JH, Greiner A (2003) Adv Mater 15:1929–1932
13. Prokop A, Helling H-J, Hahn U, Udomkaewkanjana C, Rehm KE (2005) Clin Orthop Relat Res 432:226–233
14. Auras R, Harte B, Selke S (2004) Macromol Biosci 4:835–864
15. Devassine M, Henry F, Guerin P, Briand X (2002) Int J Pharm 242:399–404
16. Rasselet D, Ruellan A, Guinault A, Miquelard-Garnier G, Sollogoub C, Fayolle B (2014) Eur Polym J 50:109–116
17. Bocchini S, Frache A (2013) Express Polym Lett 7:431–442
18. Zhang X, Espiritu M, Bilyk A, Kurniawan L (2008) Polym Degrad Stab 93:1964–1970
19. Qiu Z, Pan H (2010) Compos Sci Technol 70:1089–1094
20. Kikkawa Y, Abe H, Iwata T, Inoue Y, Doi Y (2002) Biomacromolecules 3:350–356
21. Tsuji H, Miyauchi S (2001) Polym Degrad Stab 71:415–424
22. Aoyagi Y, Yamashita K, Doi Y (2002) Polym Degrad Stab 76:53–59
23. Wachsen O, Platkowski K, Reichert K-H (1997) Polym Degrad Stab 57:87–94
24. Opaprakasit P, Opaprakasit M, Tangboriboonrat P (2007) Appl Spectrosc 61:1352–1358
25. Opaprakasit P, Opaprakasit M (2008) Macromol Symp 264:113–120

26. Hsu ST, Yao YL (2014) J Manuf Sci Eng Trans ASME 136:021006-1–021006-9
27. Tabi T, Sajó I, Szabó F, Luyt A, Kovács J (2010) Express Polym Lett 4:659–668
28. Nugroho P, Mitomo H, Yoshii F, Kume T (2001) Polym Degrad Stab 72:337–343
29. Milicevic D, Trifunovic S, Galovic S, Suljovrujic E (2007) Radiat Phys Chem 76:1376–1380
30. Montanari L, Cilurzo F, Selmin F, Conti B, Genta I, Poletti G, Orsini F, Valvo L (2003) J Controll Release 90:281–290
31. Hsu S-T, Tan H, Yao YL (2012) Polym Degrad Stab 97:88–97
32. Copinet A, Bertrand C, Govindin S, Coma V, Couturier Y (2004) Chemosphere 55:763–773
33. Yasuda N, Wang Y, Tsukegi T, Shirai Y, Nishida H (2010) Polym Degrad Stab 95:1238–1243
34. Nakayama N, Hayashi T (2007) Polym Degrad Stab 92:1255–1264
35. Wang WW, Man CZ, Zhang CM, Jiang L, Dan Y, Nguyen TP (2013) Polym Degrad Stab 98:885–893
36. Man C, Zhang C, Liu Y, Wang W, Ren W, Jiang L, Reisdorffer F, Nguyen TP, Dan Y (2012) Polym Degrad Stab 97:856–862
37. Fischer EW, Sterzel HJ, Wegner G (1973) Kolloid Z Z Polym 251:980–990
38. Pan P, Zhu B, Kai W, Dong T, Inoue Y (2008) Macromolecules 41:4296–4304
39. Pan P, Kai W, Zhu B, Dong T, Inoue Y (2007) Macromolecules 40:6898–6905
40. Socrates G (1994) Infrared characteristic group frequencies: tables and charts. Wiley, New York
41. Gardette M, Thérias S, Gardette J-L, Murariu M, Dubois P (2011) Polym Degrad Stab 96:616–623
42. Meaurio E, López-Rodríguez N, Sarasua JR (2006) Macromolecules 39:9291–9301
43. Petchsuk A, Submark W, Opaprakasit P (2013) Polym J 45:406–412
44. Fulmer GR, Miller AJ, Sherden NH, Gottlieb HE, Nudelman A, Stoltz BM, Bercaw JE, Goldberg KI (2010) Organometallics 29:2176–2179